Transcriptome Profile of Human Colorectal Adenomas

Jacob Sabates-Bellver,[1] Laurens G. Van der Flier,[4] Mariagrazia de Palo,[5] Elisa Cattaneo,[1] Caroline Maake,[2] Hubert Rehrauer,[3] Endre Laczko,[3] Michal A. Kurowski,[9] Janusz M. Bujnicki,[9] Mirco Menigatti,[7] Judith Luz,[8] Teresa V. Ranalli,[6] Vito Gomes,[6] Alfredo Pastorelli,[5] Roberto Faggiani,[5] Marcello Anti,[5] Josef Jiricny,[1] Hans Clevers,[4] and Giancarlo Marra[1]

[1]Institute of Molecular Cancer Research, [2]Institute of Anatomy, and [3]Functional Genomic Center, University of Zurich, Zurich, Switzerland; [4]Hubrecht Institute, Netherlands Institute for Developmental Biology, Utrecht, the Netherlands; [5]Gastroenterology Unit and [6]Pathology Department, Belcolle Hospital, Viterbo, Italy; [7]Institute of Biochemistry and Genetics and [8]Division of Medical Genetics, University of Basel, Basel, Switzerland; and [9]Laboratory of Bioinformatics and Protein Engineering, International Institute of Molecular and Cell Biology, Warsaw, Poland

Abstract

Colorectal cancers are believed to arise predominantly from adenomas. Although these precancerous lesions have been subjected to extensive clinical, pathologic, and molecular analyses, little is currently known about the global gene expression changes accompanying their formation. To characterize the molecular processes underlying the transformation of normal colonic epithelium, we compared the transcriptomes of 32 prospectively collected adenomas with those of normal mucosa from the same individuals. Important differences emerged not only between the expression profiles of normal and adenomatous tissues but also between those of small and large adenomas. A key feature of the transformation process was the remodeling of the Wnt pathway reflected in patent overexpression and underexpression of 78 known components of this signaling cascade. The expression of 19 Wnt targets was closely correlated with clear up-regulation of *KIAA1199*, whose function is currently unknown. In normal mucosa, KIAA1199 expression was confined to cells in the lower portion of intestinal crypts, where Wnt signaling is physiologically active, but it was markedly increased in all adenomas, where it was expressed in most of the epithelial cells, and in colon cancer cell lines, it was markedly reduced by inactivation of the β-catenin/T-cell factor(s) transcription complex, the pivotal mediator of Wnt signaling. Our transcriptomic profiles of normal colonic mucosa and colorectal adenomas shed new light on the early stages of colorectal tumorigenesis and identified *KIAA1199* as a novel target of the Wnt signaling pathway and a putative marker of colorectal adenomatous transformation.

(Mol Cancer Res 2007;5(12):1263–75)

Introduction

In developed countries, sporadic adenomatous colorectal polyps are found in roughly one third of asymptomatic adults below the age of 50 who undergo colonoscopy. Depending on their characteristics (multiplicity, size, histologic features, and degree of dysplasia), these lesions can be associated with a substantial risk of recurrence (up to 60% at 3 years) and the development of advanced neoplastic disease (reviewed in ref. 1 and references therein). It has been estimated that 15% of all adenomas measuring ≥1 cm will progress to carcinomas within 10 years of their detection (2).

Although adenomatous polyps are not the only precancerous lesions in the colorectum, they are the most common, and they are the precursors of most of the cancers in this organ. In these neoplasms, the transformation process begins in the epithelial crypts and seems to result from qualitative, quantitative, and spatial subversion of the Wnt signaling pathway, the physiologic regulator of epithelial homeostasis (3-5). This adenoma-carcinoma pathway of tumorigenesis is characterized by mutations involving various components of this pathway (e.g., *APC*, whose germ-line mutations are responsible for familial adenomatous polyposis; *CTNNB1*, which encodes a subunit of the cadherin protein complex known as β-catenin; and *Axin*, the gene encoding a multidomain scaffold protein that is essential for β-catenin degradation). The result of these mutations is an accumulation of β-catenin, first in the cytoplasm and then in the nucleus, where it associates with DNA-binding proteins of the T-cell factor (TCF)/lymphoid enhancer factor family, transforming them from transcriptional repressors into transcriptional activators that affect the expression of numerous genes involved in epithelial homeostasis.

Although the key role played by adenomatous polyps in colorectal tumorigenesis is widely acknowledged, the gene expression changes that trigger or accompany their development

Received 6/9/07; revised 7/28/07; accepted 8/2/07.
Grant support: Zurich Cancer League and Swiss National Science Foundation. The costs of publication of this article were defrayed in part by the payment of page charges. This article must therefore be hereby marked *advertisement* in accordance with 18 U.S.C. Section 1734 solely to indicate this fact.
Note: Supplementary data for this article are available at Molecular Cancer Research Online (http://mcr.aacrjournals.org/).
J. Sabates-Bellver and L.G. Van der Flier contributed equally to this work.
Requests for reprints: Giancarlo Marra, Institute of Molecular Cancer Research, University of Zurich, Winterthurerstrasse 190, 8057 Zurich, Switzerland. Phone: 41-044-635-3472; Fax: 41-044-635-3484. E-mail: marra@imcr.uzh.ch

doi:10.1158/1541-7786.MCR-07-0267

have never been comprehensively studied. We therefore conducted a transcriptomic analysis of prospectively collected colorectal adenomas using a standardized oligonucleotide microarray covering the entire human genome. This study not only provided new information that is fundamental for future molecular characterization of these precancerous lesions but also allowed us to identify a putative marker of colorectal tumorigenesis.

Results

The focus of our study was the adenoma-adenocarcinoma pathway of colorectal carcinogenesis, which is closely linked to deregulation of the Wnt signaling pathway. To gain insight into the early steps of this process, we confined our investigation exclusively to sporadic, pedunculated colorectal adenomas (type 0-Ip of the Paris classification; ref. 6). Nonpolypoid and sessile polypoid lesions were not included because in some cases their transformation is believed to proceed along nonadenomatous pathways (7). Details on our case selection criteria are provided in Materials and Methods.

Thirty-two pedunculated adenomatous polyps, each with matched samples of normal mucosa, were prospectively collected from 28 patients (Table 1). The total number of synchronous and previously excised adenomas was <3 in 18 of 28 patients and 3 to 15 in the remaining 10. In this latter subgroup, the absence of *APC*- or *MYH*-associated multiple adenomatosis had been confirmed by genetic testing of lymphocyte DNA. Histologic analysis of one polyp (case NM) revealed superficial infiltration of the submucosa, but this case was not excluded because the region sampled for microarray analysis was clearly adenomatous. (As noted below, this finding was consistent with the results of hierarchical cluster analysis shown in Supplementary Fig. S1.).

Analysis of microarray data for the 32 adenoma/normal mucosa tissue pairs revealed that 31,033 of the probes were expressed in one or both of the tissue groups. The normal tissues were effectively segregated from the adenomas in four unsupervised analyses of the expression levels of these genes [hierarchical clustering, principal component analysis (PCA), correlation analysis, and correspondence analysis (CA); see Materials and Methods for details; Fig. 1]. In a separate

Table 1. Characteristics of the 28 Patients with Adenomatous Polyps Included in the Study

Patient	Age (y)	Sex	Colon segment involved	Maximum adenoma diameter (mm)	Microscopic appearance	Highest degree of dysplasia in the adenoma*	Degree of dysplasia at sampling site*	No. adenomas at study colonoscopy †	No. previously excised adenomas ‡	No. previous and/or synchronous hyperplastic polyps	Familiarity for colorectal cancer (relative, onset age)
GL§	49	M	D/S	10/10	T-V/T-V	H/L	H/L	9	4‖,¶	15**	Mother, 70
PR	74	F	S	20	T-V	H	H	2	—††	0	No
PC§	69	M	S/S	10/20	T/T-V	H/H	H/H	10	—	1	No
FP§	57	M	S/S	15/30	T/T-V	H/H	H/L	1	—	1	Mother, 69
CD§	71	M	T/R	15/10	T/T	H/L	H/L	2	7‖	2	No
MA	65	M	R	15	T-V	L	L	2	—	0	No
ME	63	M	R	15	T-V	L	L	9	—	1	Father, 79
RA	64	F	A	15	T	L	L	1	7‖	0	Sister, 68
PR	72	M	R	40	T-V	H	H	5	—	0	No
SD	56	M	A	15	T	H	H	1	1‖	0	Mother, 83; sister, 87
MP	38	M	S	15	T-V	L	L	2	—	0	Father, 79
MP	61	M	S	20	T	L	L	3	—	2	no
LG	41	M	R	20	T-V	H	L	5 (2 serrated)	—	0	Father, 60
LS	45	M	S	20	T	H	H	1	—	1	Father, 60
BG	58	M	D	15	T-V	L	L	2	—	1	No
PL	69	F	S	15	T-V	L	L	2	—	0	No
SMA	52	F	S	30	T	H	H	2	—	1	No
MR	58	F	D	20	T	L	L	2	—	0	No
GN	69	M	R	40	T	H	H	2	—	0	No
BA	69	M	S	30	T	L	L	6	—	0	No
PF	56	M	S	30	T	L	L	2	—	0	No
RC	55	F	A	30	T-V	L	L	12	3‖,¶	1	No
TMA	58	F	S	10	T	L	L	1	—	0	Mother, 85
NM	52	M	R	35	T-V	T1 ‡‡	H	1	—	0	No
MA	83	M	S	10	T-V	H	H	2	—	1	No
MM	50	M	S	30	T-V	H	H	2	—	0	Father's brother, 65
NF	79	M	A	20	T-V	L	L	2	—	0	Mother, 70
PN	67	F	S	15	T-V	L	L	1	—	1	No

Abbreviations: M, male; F, female; A, ascending colon; T, transversum; D, descending colon; S, sigmoid colon; R, rectum; T, tubular; T-V, tubulovillous; L, low-grade dysplasia; H, high-grade dysplasia.

*Low-grade versus high-grade dysplasia as defined by the WHO classification of tumors of the digestive system, editorial and consensus conference in Lyon, France, November 6-9, 1999. IARC.

† This number includes the adenoma(s) subjected to microarray analysis.

‡ Total number of adenomas detected and excised during previous colonoscopies.

§ Two adenomas from these patients were analyzed.

‖ These cases were considered as recurrent adenomas for the CCA.

¶ The index colonoscopy was done in a different center about 10 y before the study colonoscopy.

** Hyperplastic polyposis.

†† No previous colonoscopies.

‡‡ Superficial submucosal invasion (T1). The tissue collected for microarray came from the adenomatous portion of the polyp.

analysis, these two tissue groups were also unequivocally distinguished from a previously described set of 25 colon cancers (8), which we reanalyzed for this study with the same microarray used to characterize the adenomas and normal mucosa (Supplementary Fig. S1).

Almost half of the expressed probes (15,059 of 31,033) displayed significant expression changes in adenomas. Those with fold changes ≥2 (1,190 probes up-regulated and 2,469 down-regulated in adenomas) were subjected to gene ontology analysis to identify the biological processes involved in the transition of normal mucosa to adenoma. The most significant results of this analysis are listed in Supplementary Table S1. The processes that were most markedly overrepresented among genes that were up-regulated in adenomas included mitosis, DNA replication, and spindle organization. Down-regulated genes were predominantly involved in host immune defense, inorganic anion transport, organ development, and inflammatory response, although a small group of genes involved in the latter process was up-regulated in adenomas (Supplementary Fig. S2).

We then analyzed the transcript levels of 319 genes believed to be components of the complex Wnt signaling pathway (Supplementary Table S2). Sixty-six of these genes (21%) were not expressed in either the normal or adenomatous tissue, and 34% were expressed similarly in both tissue groups. The remaining 144 genes displayed significantly altered expression in adenomas, and 78 of 144 displayed fold changes of ≥2.

A supervised extension of CA (9), canonical CA (CCA), was then used to identify possible correlations between gene expression patterns and clinical or pathologic variables. Four of the variables considered (adenoma diameter, colon segment of origin, degree of dysplasia, and adenoma recurrence; see Table 1) were clearly associated with distinct clusters of expression profiles (Fig. 2, variables in A and clusters for adenoma diameter in B; more details in the legend to this figure). The profile of adenomas measuring >20 mm could be easily distinguished from those of smaller (≤20 mm) adenomas. As shown by CCA and visualized on the corresponding CCA score plot (Fig. 2B), the centers of the three adenoma size clusters are distributed along the principal CCA axis (the vertical axis in Fig. 2B, the most important axis of separation of the expression profiles) in a definite order, with increasing diameters corresponding to progressively higher CCA scores. The variable large adenoma diameter was closely correlated with the vertical CCA axis (i.e., its vector "d>20mm" in Fig. 2A is almost parallel to this axis). It is interesting to note that the same correlation can be observed for the variable high-degree dysplasia (i.e., represented in Fig. 2A by vector "Hd"). This finding confirms the expected correlation between larger diameters and higher-degree dysplasia.

The CCA plot of the 11,709 modeled probes (loading plot, not shown) suggested that the distinction between the three size groups of adenomas is due to a complex network of relatively small changes in the expression of numerous genes (as opposed to marked changes involving a limited number of genes). Nevertheless, to maximize the use of the extensive data sets, we selected the 500 probes with the highest loading scores along the CCA axis 1 and isolated a set of genes whose expression changes displayed significant positive or negative correlation with adenoma size (Supplementary Table S3). Although their association with adenomas must be validated in a larger series, these are the expression changes most likely to play causal roles in the progression of these tumors.

It should be mentioned that normal mucosa from the sigmoid colon had an expression profile that differed significantly from that of tissues from other colon segments (Fig. 2A). This finding will be explored in a future study conducted on a large series of normal mucosa samples from different colorectal segments.

The transcriptional profile of the 32 adenomas was thoroughly analyzed to identify genes likely to be involved in the development and evolution of these lesions. One of the first features that attracted our attention was the marked up-regulation of *KIAA1199* (Supplementary Table S4), a gene encoding a protein with unknown function. Its overexpression was striking in all colorectal adenomas we examined (average increases of 54.8-fold compared with normal mucosa) and in carcinomas (8). These findings were fully confirmed by real-time reverse transcription-PCR analysis of RNA extracted from samples used for the microarray study and from additional samples collected after the present study was completed (Supplementary Fig. S3).

In light of these findings, it was natural to wonder whether *KIAA1199* might be a novel positively regulated target of Wnt signaling, which is characteristically deregulated in colorectal tumors. Previous microarray studies indicated that genes coregulated at the transcriptional level under different conditions tend to be involved in the same processes and pathways, and the analysis of transcriptional coexpression has been used to predict the function of novel genes (10-12). Therefore, we conducted a search for known Wnt targets (listed in Supplementary Table S5) among the genes whose expression patterns in all the tissue samples significantly correlated with those of *KIAA1199*. (The procedure used in this analysis is summarized in Materials and Methods and Supplementary Fig. S4.) Forty-nine percent of the known Wnt targets that were overexpressed in our adenoma samples had expression patterns that were positively correlated with that of *KIAA1199* (Fig. 3A and B) as opposed to only 7.9% of the overexpressed genes that are not considered Wnt targets ($P < 0.0001$).

Evidence of the potential involvement of *KIAA1199* in the Wnt signaling pathway had also emerged from another study by our group (13). A combined analysis of microarray data of tissues and cell lines placed *KIAA1199* at the top of a list of genes [Supplementary Table S1 of ref. 13] that were up-regulated in colorectal adenomas and down-regulated in colon cancer cell lines that had undergone stable transfection with doxycycline-inducible forms of dominant-negative TCF1 or TCF4 to suppress Wnt signaling (14, 15). In the present study, *KIAA1199* was also found to be markedly down-regulated in LS174T colon cancer cells in which Wnt signaling had been blocked by the induction of β-catenin small interfering RNA or NH_2-terminal–deleted TCF4 (15, 16). The dramatic decrease in *KIAA1199* mRNA levels associated with this inhibition of the Wnt pathway was confirmed by Northern blotting (Fig. 3C).

In general, Wnt target genes are expressed predominantly in the proliferating compartment of normal intestinal crypts (lower portion), and their expression is appreciably increased in

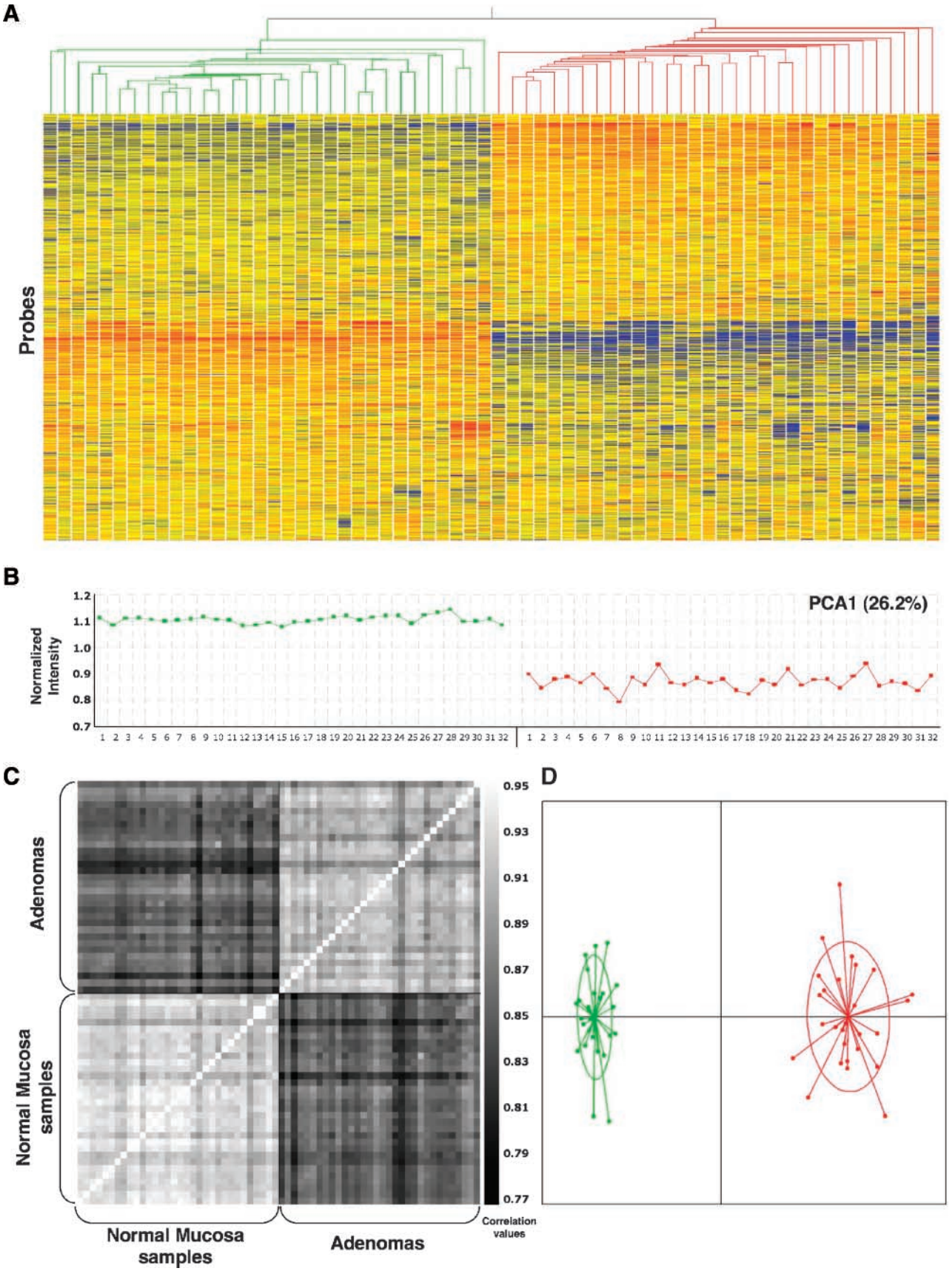

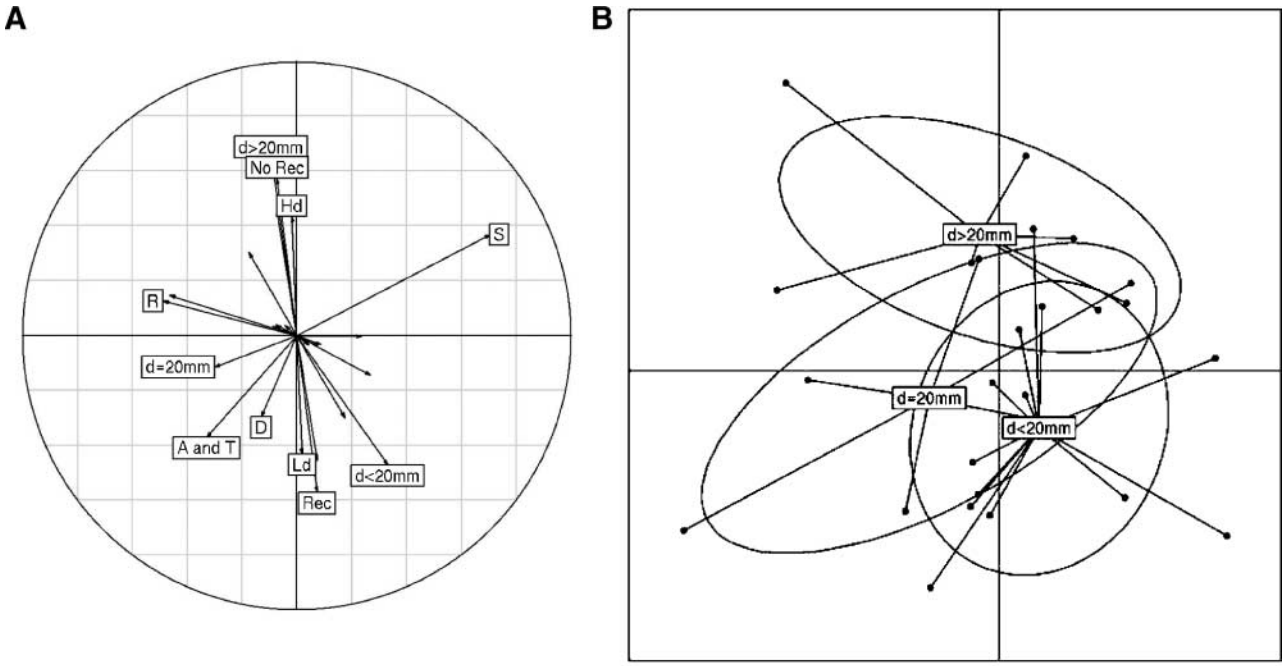

FIGURE 2. Clinical/pathologic variables that correlate with distinct gene expression profiles. The panels summarize the most important results of the CCA of mRNA intensity log-ratio values (adenoma: normal) of expressed genes. For clarity, CCA axis 1 has been drawn vertically in both panels. **A.** Correlation between specific clinical/pathologic variables (adenoma diameter, colon segment of origin, degree of dysplasia, and adenoma recurrence) and clusters of differential gene expression profiles (coded as log-ratio profiles), such as those shown in **B**. Each vector represents a specific value for a given variable (e.g., adenoma diameter of >20 mm and high-degree dysplasia) and points toward the center of the profile cluster correlated with the clinical/pathologic characteristic it represents. If the centers for each specific value are separated, the corresponding vectors point in distinct directions; otherwise, they are directed toward the same point. In the former case, the represented variable can be assumed to be significantly correlated with the profiles; in the latter case, there is no correlation. The length of the vector reflects the strength of the correlation: those approaching the circumference of the correlation circle, which represents a correlation value of 1, indicate stronger correlation than shorter vectors (correlation closer to 0). d, diameter; Hd, high-degree dysplasia; Ld, low-degree dysplasia; A, ascending colon; T, transverse colon; D, descending colon; S, sigmoid colon; R, rectum; Rec, recurrent adenomas; no Rec, no recurrent adenomas. Unlabeled vectors are related to variables that were not clearly associated with any distinct cluster of expression profiles. Larger adenomas were predictably associated with high-degree dysplasia. In contrast, their association with nonrecurrence was unexpected and probably due to the fact that patients who had already undergone endoscopic polypectomy (i.e., those with recurrence) presented relatively recent-onset (consequently, smaller) polyps at the study colonoscopy. **B.** CCA score plot with samples grouped by adenoma diameter. Each of the three size-related groups is delimited by an ellipse with the center labeled. The ellipse representing the adenomas measuring >20 mm in diameter shows very little overlap with those of the other two groups (adenomas with diameters of 20 mm and those with diameters of <20 mm).

adenomatous glands (15). Our analysis of human tissues with preserved architecture indicated that these are also attributes of *KIAA1199*. In *in situ* hybridization studies, *KIAA1199* mRNA was detectable only in the lower portion of normal colonic epithelial crypts (Fig. 4A and B), and its expression levels were much higher in dysplastic glands (Fig. 4C). These patterns were confirmed at the protein level by immunohistochemistry done with an antibody raised in our laboratory (Fig. 4D-J). This analysis also revealed that the KIAA1199 is a cytoplasmic protein whose expression is most intense near the cell membrane, particularly on the luminal side of the dysplastic cell multilayer (Fig. 4F-J).

FIGURE 1. Unsupervised analyses of microarray data. **A.** Hierarchical clustering analysis. The 64 tissue samples represented on the *X* axis include 32 normal mucosal samples (*green branches*) and 32 adenomas (*red branches*). Each probe plotted on the *Y* axis is color coded to indicate the level of expression of the gene relative to its median expression level across the entire tissue sample set (*blue*, low; *red*, high). In the adenoma dendrogram, branches representing individual samples and small groups merge at higher levels than those of the normal mucosa dendrogram, reflecting lower-level correlation (i.e., higher variability among the adenoma specimens). **B.** PCA. Profile plot of the normalized first principal component (*PCA1*) across the 64 specimens (*green dots*, normal mucosa; *red dots*, adenomas). The two tissue groups differ significantly in terms of PCA1 ($P < 0.0001$), which accounted for 26% of the total variance. Note the higher variability of the PCA1 values in the adenoma group (higher fluctuation). **C.** Correlation analysis. Tile plot visualization of the pairwise correlations of the samples. Correlation values are indicated on the grayscale column (*white* > *black*: high > low). High correlation is observed among the samples within each group (*top right quadrant*, adenomas; *bottom left quadrant*, normal mucosa), although the adenomas displayed somewhat greater diversity (i.e., on the whole, the gray tones in the *top right quadrant* are darker than those in the *bottom left quadrant*). Top left and bottom right quadrants, normal and adenoma samples are poorly correlated. However, samples from the same patient generally showed higher correlation than that observed between normal and adenoma samples from different patients (bright pixels on the secondary diagonals in the *top left* and *bottom right quadrants*). This finding probably reflects the strong influence of several factors, including the individual genetic background and lifestyle and the fact that the normal and adenomatous tissues from a given patient were from the same colon segment. **D.** CA of mRNA log(intensity) values of expressed genes from 27 of the 32 tissue pairs (*green dots*, normal mucosa; *red dots*, adenoma). The other five pairs were excluded from this analysis because one of the two samples behaved as an outlier. Limiting our analysis to the more homogeneous pairs facilitated the comparison of the gene expression profiles for the two tissue groups and allowed more reliable identification of clinical/pathologic variables associated with profile scatter (see Fig. 2). The areas delimited by the ellipses represent 95% of the estimated binormal distribution of the sample scores on the first and second CA axes. The map of the sample scores on the first two axes shows that CA efficiently discriminates between normal and adenoma samples. Higher variability is evident in the adenoma group, where the samples are more widely dispersed.

Discussion

Adenomatous colorectal polyps are one of the most common human tumors and the most frequent precancerous lesions in the colorectum, but their transcriptome has been only partially analyzed, and the data are generally based on a limited number of cases (17-20). We attempted to fill this gap by doing a comprehensive whole-genome microarray analysis of a large, highly homogenous set of adenomas that was collected prospectively.

A comparison of the transcriptomes of adenomatous polyps and segment-matched samples of normal colorectal mucosa revealed evidence of broad-scale remodeling. As a starting point for future verification studies, we have drawn up a list of 478 genes that were significantly up-regulated (n = 153) or down-regulated (n = 325) in the adenomatous tissues (fold changes of ≥4; Supplementary Table S4). Space constraints preclude more than a cursory examination of this list, but we have highlighted in Table 2 certain aspects that we feel are particularly interesting in terms of their relevance to the process of adenoma formation. For instance, transcription regulation seems to be extensively modified. Twenty-nine molecules involved in this process were expressed in adenomas at levels

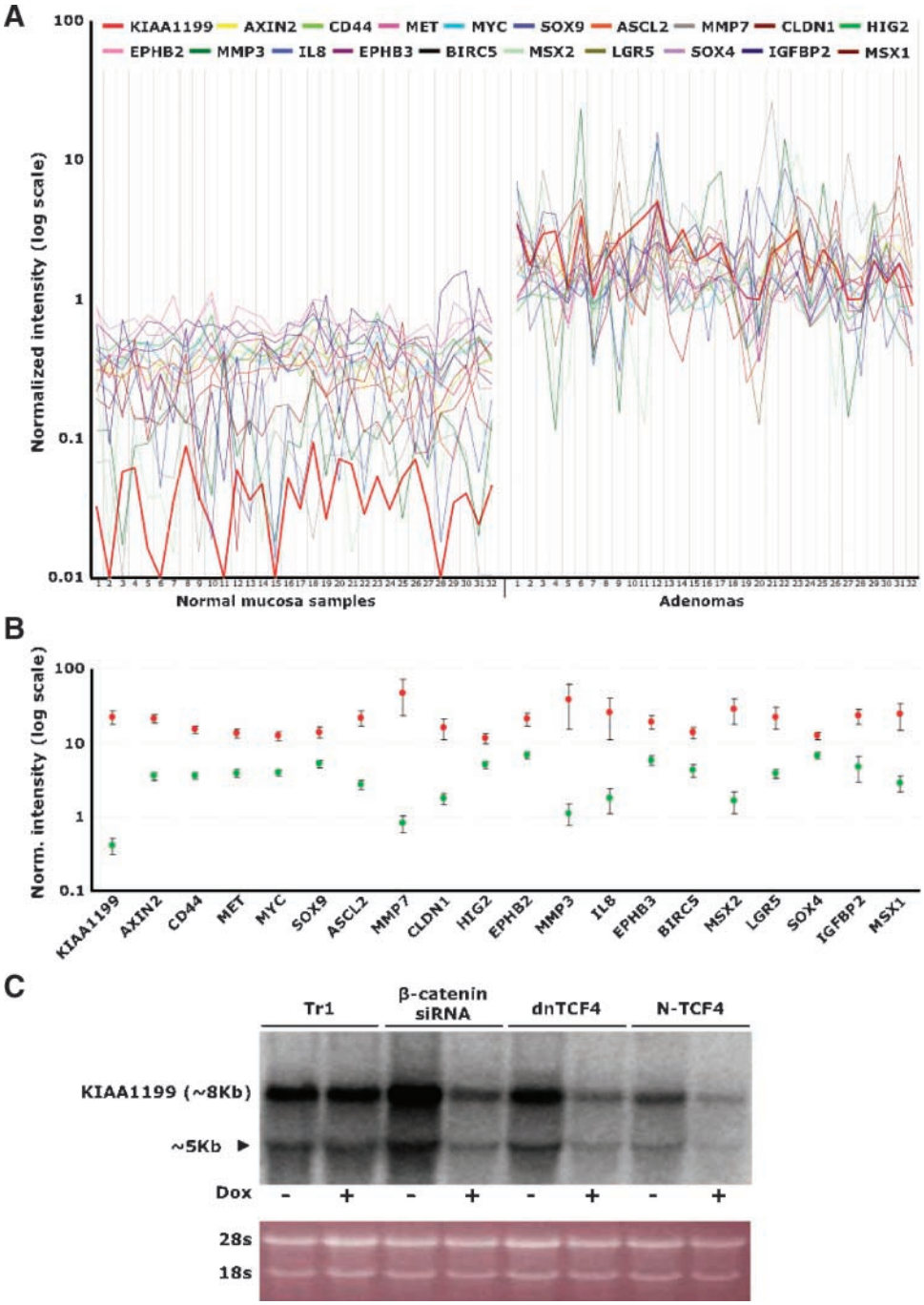

FIGURE 3. *KIAA1199* is a putative target of Wnt signaling. **A.** Degree of correlation between the expression of *KIAA1199* mRNA and that of 19 known Wnt signaling target genes identified with the procedure described in Materials and Methods, Results, and Supplementary Fig. S4. For each of the 20 genes, the graph shows the normalized intensity of expression level (plotted on the *Y axis*) in each of the 32 adenomas and corresponding samples of normal mucosa (*X axis*). **B.** Mean expression of each gene in normal mucosa (*green dots*) and adenomas (*red dots*). Bars, confidence interval. **C.** Northern blot showing reduced *KIAA1199* expression in LS174T cells following doxycycline-mediated induction of β-catenin small interfering RNA, dominant-negative TCF4 (*dnTCF4*), or NH_2-terminal–deleted TCF4 (*N-TCF4*). The ~8-kb band corresponds to full-length *KIAA1199* mRNA. The lower band (~5 kb) may represent an alternative form of this mRNA. Dox, cell transfectants grown in the presence or absence of doxycycline; Tr1, a parental clone (i.e., cells expressing the repressor protein modified by doxycycline but not transfected with β-catenin small interfering RNA, dominant-negative TCF4, or NH_2-terminal–deleted TCF4) used as a control of doxycycline exposure. Bottom, ethidium bromide–stained agarose gel as a loading control.

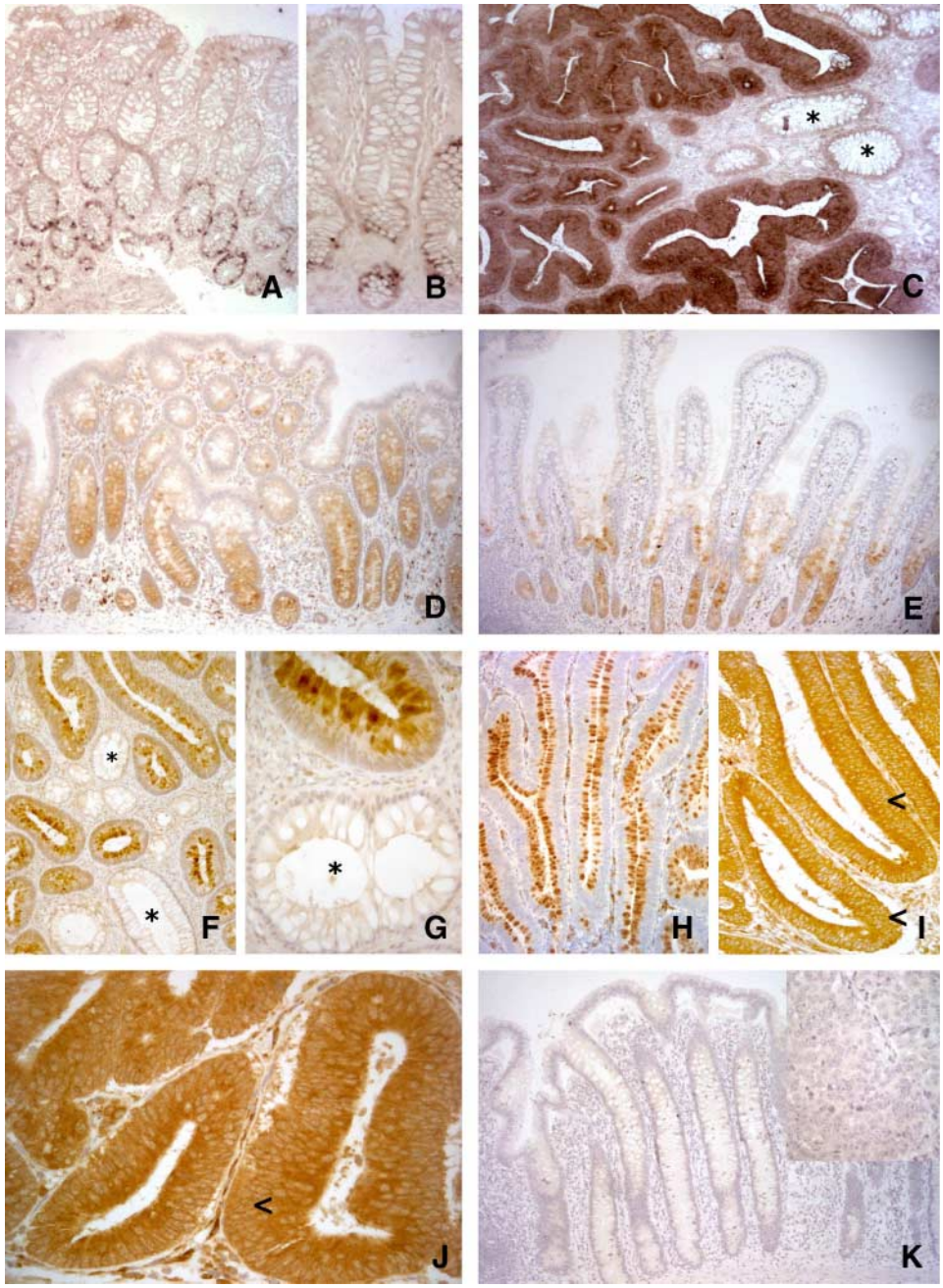

FIGURE 4. Expression of KIAA1199 mRNA and protein in normal intestinal mucosa and colorectal tumors. *In situ* hybridization studies (**A-C**) localized *KIAA1199* mRNA expression to the lower portion of normal epithelial crypts (**A** and **B**) and revealed that expression is markedly up-regulated in colorectal tumors (**C**). Asterisk, note the different levels of expression in tumor glands and normal crypts. **D.** KIAA1199 protein expression is also limited to the lower half of the normal colonic crypts, and a similar pattern is observed in the ileal mucosa (**E**), where the protein is expressed only in the crypts (not in the villi). In **F** and **G**, adenomatous crypts with low-grade dysplasia present increased expression of KIAA1199, particularly in the cytoplasm facing the crypt lumen, and in and around the mucin vacuoles of goblet cells (note the striking difference with goblet cells of normal crypts in both panels). The expression pattern changes dramatically during the transition from low-grade dysplasia with goblet cell differentiation (**H**) to high-grade dysplasia in which this differentiation is no longer apparent. **J.** In more advanced colon tumors, KIAA1199 overexpression is maintained. Note that, in **I** and **J**, the expression of KIAA1199 protein (like that of *KIAA1199* mRNA; **C**) is highest in the luminal portion of the dysplastic glands (*arrowheads*, multilayer of unstained nuclei occupying more than the basal half of the dysplastic epithelium). **K.** Normal mucosa, with the corresponding tumor in the inset. Negative control: KIAA1199 antibody preabsorbed with the peptide used to immunize rabbits.

>4 higher or lower than those observed in the normal mucosa, but there were also several smaller changes in this category (Supplementary Table S6) that might also have dramatic effects on gene expression. Several other alterations reported in Table 2 are noteworthy in terms of their potential effect on cell proliferation, differentiation, apoptosis, and cell adhesion: (*a*) up-regulation of four members of the REG (regenerating) family of genes (21, 22), which would lead to increased tissue mitogen expression; (*b*) up-regulation of *LCN2* (23) and down-regulation of *ZFHX1B/SIP-1* (24) in the absence of significant changes in the expression of the epithelial cadherin *CDH1* (E-cadherin), which would prevent or delay the epithelial-mesenchymal transition [changes were also noted in the expression of other cell adhesion genes of the cadherin and claudin families, including the striking overexpression of the placental cadherin gene *CDH3*, which is associated with early events in the transformation process (25, 26)]; (*c*) down-regulation of *ZFHX1B/SIP-1* and *Max dimerization protein 1* (*MXD1/MAD1*; decreased only 3.3-fold and therefore not listed in Table 2; refs. 27, 28) and overexpression of the *RTEL1* helicase, which should facilitate telomere elongation (29); (*d*) alterations that would diminish apoptosis [e.g., overexpression of the decoy receptor for Fas ligand, *TNFRSF6B*, which is reportedly coregulated with *RTEL1* on chromosome 20q13.3

Table 2. Genes Most Likely to be Involved in the Development and Evolution of Colorectal Adenomas (A Subset of Genes Listed in Supplementary Table S4) Subdivided by Gene Ontology Category

Gene symbol	Gene name	Fold differences*	
		▲	▼
Regulation of transcription			
NLF1	Nuclear localized factor 1	33.1	
FOXQ1	Forkhead box Q1	24.4	
MSX2	Msh homeobox homologue 2	22.2	
ASCL2	Achaete-scute complex-like 2	17.3	
MSX1	Msh homeobox homologue 1	8.5	
IRX3	Iroquois homeobox protein 3	8.4	
GRHL3	Grainyhead-like 3	7.9	
TRIM29	Tripartite motif-containing 29	7.4	
ETV4	Ets variant gene 4 (E1A enhancer binding protein, E1AF)	5.4	
ARNTL2	Aryl hydrocarbon receptor nuclear translocator-like 2	5.3	
TEAD4	TEA domain family member 4	5.2	
SP5	Sp5 transcription factor	5.2	
HES6	Hairy and enhancer of split 6	4.6	
TBX3	T-box 3	4.6	
NFE2L3	Nuclear factor (erythroid-derived 2)-like 3	4.3	
GRHL1	Grainyhead-like 1	4.2	
FEV	FEV (ETS oncogene family)		15.1
SPIB	Spi-B transcription factor		13.2
NEUROD1	Neurogenic differentiation 1		10.6
MEIS1	Meis1, myeloid ecotropic viral integration site 1		7.1
NR3C1	Nuclear receptor subfamily 3, group C, member 1		5.9
NR5A2	Nuclear receptor subfamily 5, group A, member 2		5.6
THRB	Thyroid hormone receptor, β		5.2
ZNF483	Zinc finger protein 483		5.1
ZFHX1B	Zinc finger homeobox 1b (SIP-1)		4.8
MEOX2	Mesenchyme homeobox 2		4.7
HOXD10	Homeobox D10		4.6
MAF	v-maf musculoaponeurotic fibrosarcoma oncogene		4.5
SOX10	SRY (sex determining region Y)-box 10		4.2
Cell proliferation/differentiation/apoptosis			
REG1B	Regenerating islet-derived 1β	75.8	
REG3A	Regenerating islet-derived 3α	29.5	
TACSTD2	Tumor-associated calcium signal transducer 2	21.4	
IL-8	Interleukin-8	14.7	
SERPINB5	Serpin peptidase inhibitor, clade B, member 5 (Maspin)	13.8	
REG1A	Regenerating islet-derived 1α	8.2	
FAIM2	Fas apoptotic inhibitory molecule 2	7.5	
DUSP4	Dual specificity phosphatase 4	7.4	
REG4	Regenerating islet-derived family, member 4	6.8	
PHLDA1	Pleckstrin homology-like domain, family A, member 1	6.0	
LCN2	Lipocalin 2 (oncogene 24p3)	5.7	
RTEL1	Regulator of telomere elongation helicase 1	5.6	
TGFBI	Transforming growth factor, β induced	5.2	
IGFBP2	Insulin-like growth factor binding protein 2	4.8	
TDGF1	Teratocarcinoma-derived growth factor 1	4.7	
TNFRSF6B	Tumor necrosis factor receptor superfamily, member 6b, decoy	4.5	
DMBT1	Deleted in malignant brain tumors 1	4.2	
TNFRSF10C	Tumor necrosis factor receptor superfamily, member 10c, decoy	4.1	
ANGPTL1	Angiopoietin-like 1 (Angioarrestin)		24.9
CDKN2B	Cyclin-dependent kinase inhibitor 2B (p15, inhibits CDK4)		14.9
GPM6B	Glycoprotein M6B		11.5
ANK2	Ankyrin 2		9.8
UNC5C	Unc-5 homologue C		7.4
HPGD	Hydroxyprostaglandin dehydrogenase 15-(NAD)		6.1
CPNE8	Copine VIII		5.5
FAIM3	Fas apoptotic inhibitory molecule 3		5.4
IL6R	Interleukin-6 receptor		4.8
TUSC3	Tumor suppressor candidate 3		4.7
DUSP1	Dual specificity phosphatase 1		4.7
RERG	RAS-like, estrogen-regulated, growth inhibitor		4.6
NDN	Necdin		4.5
IGF1	Insulin-like growth factor 1 (somatomedin C)		4.0
Cell adhesion			
CDH3	Cadherin 3, type 1, P-cadherin	81.7	
CLDN2	Claudin 2	16.1	
CLDN1	Claudin 1	9.0	
DSG3	Desmoglein 3	7.3	

(*Continued on the following page*)

Table 2. Genes Most Likely to be Involved in the Development and Evolution of Colorectal Adenomas (A Subset of Genes Listed in in Supplementary Table S4) Subdivided by Gene Ontology Category (Cont'd)

Gene symbol	Gene name	Fold differences*	
		▲	▼
DSG4	Desmoglein 4	5.9	
CLDN8	Claudin 8		25.8
CDH19	Cadherin 19, type 2		8.3
CEACAM7	Carcinoembryonic antigen-related cell adhesion molecule 7		8.3
CLDN23	Claudin 23		8.0
NRXN1	Neurexin 1		7.1
PCDH19	Protocadherin 19		6.8
NLGN4X	Neuroligin 4, X-linked		6.0
TNXB	Tenascin XB		5.6
MUCDHL	Mucin and cadherin-like		5.1
PCDH9	Protocadherin 9		4.9
L1CAM	L1 cell adhesion molecule		4.2

*Overexpressed (▲) or underexpressed (▼) in adenomas (versus normal mucosa samples).

(30-32); decreased expression of the netrin-1 receptor, *UNC5C* (33); and expression changes involving three Fas apoptosis inhibitory molecules (*FAIM*), including *FAIM1*, which was increased 2.3-fold and is thus not listed in Table 2]; and (*e*) marked down-regulation of several genes that would result in reduced tumor suppression activity [e.g., those encoding the antiangiogenic factor ANGPTL1 (34), the cyclin-dependent kinase inhibitor CDKN2B/p15, and the prostaglandin catabolism enzyme HPGD (35)].

It is also important to recall the size-related differences noted in the adenoma gene expression profiles (Fig. 2; Supplementary Table S3). When validated in a larger series of tumors, these differences should provide important clues to the molecular basis of the well-known link between the dimensions and malignant potential of colorectal adenomas (1).

Our study also furnishes a complete picture of expression changes involving gene components of the Wnt pathway across the transition from normal to adenomatous epithelium (Supplementary Table S2) as well as evidence for the existence of a novel Wnt target: *KIAA1199*. This gene, which encodes a protein of unknown function, was strikingly overexpressed in all the adenomas included in this study and in 25 adenocarcinomas of the colon described in a previous report (8). Even more intriguingly, its expression was significantly correlated with that of several genes that are well-established targets of Wnt signaling. Our hypothesis that *KIAA1199* is up-regulated by the TCF(s)/β-catenin transcription complex was considerably strengthened by the marked decreases in *KIAA1199* expression observed in cultured colorectal cancer cells when the Wnt pathway was inhibited by overexpression of dominant-negative TCF4 proteins or by β-catenin knockdown. It is not yet clear whether this is a direct effect, but this possibility is supported by the results of a recent genome-wide TCF4 ChIP-on-chip analysis, which indicates that the *KIAA1199* locus is surrounded by four TCF4-bound regions.[10] These findings are consistent with the probable role of this gene as a direct target of TCF4/β-catenin signaling in the intestine and in colorectal tumors.

Other features of *KIAA1199* expression are also compatible with its putative role as a Wnt target gene. *KIAA1199* mRNA and protein are both confined to the proliferative compartment of normal intestinal crypts, where Wnt signaling is normally active, and they are highly overexpressed in colorectal adenomas and carcinomas, where this pathway is almost always aberrantly activated.

In normal and tumor tissues, KIAA1199 is expressed in the cytoplasm of epithelial cells. In glands with low-degree dysplasia, higher concentrations are observed in the mucin vacuoles of goblet cells, but cytoplasmic expression of the protein in tumor cells remains elevated even after goblet cell differentiation has been lost (Fig. 4). These features, together with the localization of KIAA1199 in the luminal portion of the cytoplasm, are suggestive of a secreted and/or membrane protein. This conclusion is consistent with our *in silico* analysis of KIAA1199 (see Supplementary Data and Supplementary Fig. S5), which strongly predicts the presence of a signal peptide at its NH_2-terminal end. In addition, the central region of KIAA1199 contains a TMEM2 homology domain, which is present in several eukaryotic proteins, including TMEM2, polyductin (PKHD1), and fibrocystin L (PKHD1L1; Fig. 5), all large receptor proteins characterized by an NH_2-terminal signal peptide or a single transmembrane helix and a short cytoplasmic tail (36).

A study based on yeast two-hybrid screens suggested that KIAA1199 may interact with plexin A2 (KIAA0463; ref. 37). The transmembrane plexins interact with transmembrane semaphorins on nearby cells, providing "stop" and "go" signals that are crucial for cell motility and invasive growth (38, 39). KIAA1199/plexin A2 interaction could thus play important roles in colorectal tumorigenesis not only in the invasive stages but also earlier during the formation of abnormal glands in benign adenomas.

A recent report linked high levels of *KIAA1199* mRNA with cell mortality in human fibroblasts and in a renal cell carcinoma cell line (40). In that study, however, there was no significant increase in *KIAA1199* expression during replicative aging of mortal cells, and this finding contrasts with the documented behavior of other genes involved in cell aging (41). Furthermore,

[10] Hatzis et al., unpublished data.

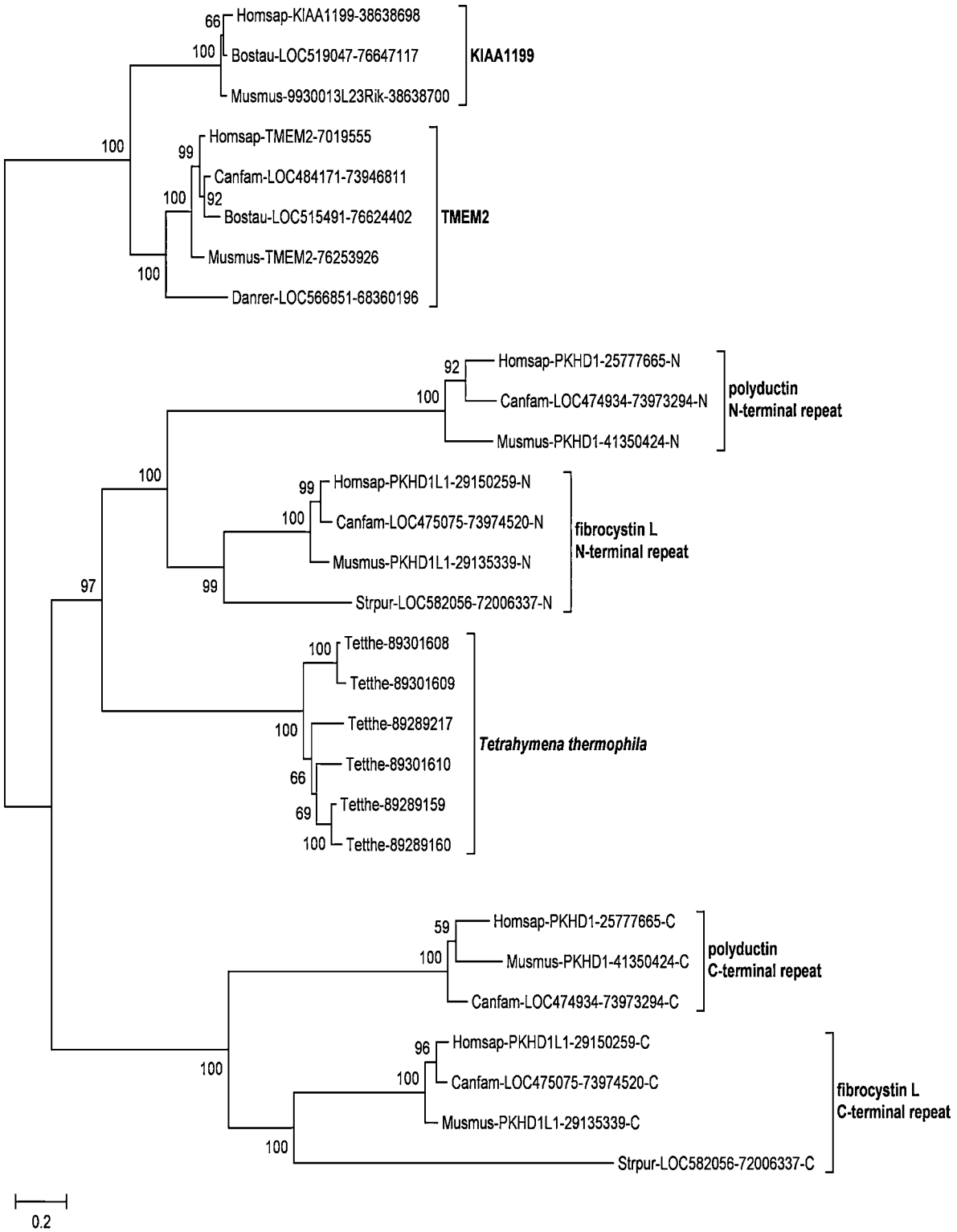

FIGURE 5. Phylogenetic tree of the proteins containing the TMEM2 homology domain found in the central region of KIAA1199. The tree was generated with MEGA3 (52) from the multiple sequence alignment shown in Supplementary Fig. S5. It was calculated with the minimum evolution algorithm and the JTT matrix. Positions with gaps were removed for calculation of pairwise distances. Node robustness was assessed using the bootstrap method with 100 resamplings. (Bootstrap values are shown at the nodes.) Two branches emerged, one comprising KIAA1199 and TMEM2 and the other with polyductin, fibrocystin L, and several other THD-containing proteins found in the ciliate *Tetrahymena thermophila*, which were apparently generated in a series of *Tetrahymena*-specific gene duplications. The NH_2-terminal repeats of polyductin and fibrocystin L clustered together, as did the COOH-terminal repeats, suggesting that the intragenic duplication of the TH domain in the ancestor of polyductin and fibrocystin L occurred before the divergence of chordates and echinoderms (more details in Supplementary Data).

the authors reported wide variation in *KIAA1199* mRNA expression in breast cancer cell lines, and this finding raises the possibility that expression of this gene *in vivo* and in cell lines may differ.

We believe that our microarray data will serve as a springboard and reference point for other studies on the molecular basis of colorectal transformation along the adenoma-carcinoma pathway (and subsequently for the study of alternative pathways). Some of the transcriptional changes reported in this study might one day be used as molecular indices of the susceptibility of adenomas to malignant transformation, information that would be helpful in planning appropriate follow-up of the lesions. As for KIAA1199, its invariably high expression in the colorectal tumors we studied raises interesting possibilities for the development of a new molecular marker for the detection of these neoplasms. For example, because KIAA1199 expression in the normal mucosa is limited to cells in the lower portion of the crypts, which are not yet programmed to be shed into the intestinal lumen, the presence of KIAA1199 peptides in fecal water might prove to be a specific marker of adenomatous lesions. In addition, although due consideration must be given to its probable physiologic role(s) in intestinal crypts and possibly in several other human tissues (40, 42, 43), KIAA1199 may be a potential target of antibody-based therapies.

Materials and Methods

Tumor Samples

Pedunculated colorectal polyps and normal mucosa were obtained during colonoscopies carried out in the Gastroenterology Unit of the Belcolle City Hospital (Viterbo, Italy). The tissues were collected prospectively with informed patient consent and the approval of the local Human Research Ethics Committee. Patients with documented familial polyposis, with >15 adenomatous polyps (total: synchronous + previously excised; ref. 44), or currently treated with nonsteroidal anti-inflammatory drugs (including aspirin) were excluded from the study.

For each polyp, three biopsies of normal mucosa were collected from the same colon segment (≥2 cm from the site of the polyp). Immediately after removal, a small sample of epithelial tissue (5-15 mg) was cut from the tip of each polyp, leaving the underlying muscularis mucosae intact. We excluded polyps <1 cm to ensure that the sampling procedure would not interfere with the histologic diagnosis. All polyp samples were collected by a single operator (M.d.P.) using the same procedure to minimize artifacts due to sampling differences. The approach used allowed us to obtain specimens with a high percentage of epithelial cells without resorting to microdissection, which can diminish the quantity and quality of the extracted RNA.

The polyp sample and the three normal mucosal biopsies were immersed in RNAlater (Ambion) for subsequent microarray analysis, and the remainder of the polyp was submitted for pathologic analysis. The cut surface at the tip was labeled with India ink so that the sampled area could be easily identified during routine histologic examination. The tissue was then fixed in buffered formalin and embedded in paraffin. DNA extracted from sections of this specimen was also used to rule out microsatellite instability (reflecting defective DNA mismatch repair) at the *BAT26* locus, as previously described (45). All of the polyps included in the study met the following criteria: type 0-Ip (6), maximum diameter of 1 to 4 cm, absence of surface ulceration, histologic diagnosis of adenoma, and absence of microsatellite instability at *BAT26*.

In some analyses, we also included transcriptomic data from a previously described set of 25 colon cancers (mismatch repair proficient and deficient; ref. 8), which we reanalyzed for this study with the same microarray used to characterize the adenomas and normal mucosa.

Microarray Analysis, Real-time Reverse Transcription-PCR, and Northern Blotting

Total RNA was extracted (RNeasy Mini kit, Qiagen) from homogenized tissue samples (5-15 mg), and its integrity was verified by capillary gel electrophoresis (Bio Analyzer, Agilent Technologies). Complementary RNA (15 μg/sample), synthesized and labeled as previously described (8, 46), was hybridized with the Affymetrix U133 Plus 2.0 array, which contains *in situ* synthesized oligonucleotides representing the entire human genome (54,675 probes).

Raw gene expression data generated by GeneChip Operating Software (Affymetrix) were imported into the GeneSpring software program (Agilent Technologies) and normalized per chip (i.e., to the median of all values on a given array) and per gene (i.e., to the median expression level of the given gene across all samples). Analysis was done using the log expression values with GeneSpring's cross-gene error model turned on. Probes were excluded from analysis unless they were listed as "present or marginal calls" and/or had expression values ≥100 in ≥50% (≥16 of 32) of the samples in at least one of the tissue groups (adenomas and normal mucosa).

Expression data were subjected to four different unsupervised analyses: (*a*) hierarchical clustering using the Pearson correlation coefficient as a similarity measure and the average linkage algorithm for branch merging; (*b*) PCA, which reduces the dimensionality (number of variables) of a data set while retaining most of its variance (8); (*c*) correlation analysis, which involved computation of Pearson correlation coefficients for all possible sample pairs and visualization of correlation values as tile plots; and (*d*) CA, another dimension-reducing method (47), which was used to identify samples associated with particular gene expression levels. In typical CA, a matrix of *n* gene expression levels from *p* samples is treated as a two-way contingency table (genes by samples or vice versa) with *n* and *p* specifications for the "factors" gene and sample, respectively. Each intensity value thus reflects the abundance of a given transcript in a given sample. Like PCA, CA identifies independent "factorial components" that account for variance within a multidimensional gene data set, but in this case, the components are identified and ranked according to the correlation between gene and sample scores. A supervised or constrained extension of CA (9), CCA, was then used to identify possible correlations between gene expression patterns and clinical or pathologic variables. CA and CCA, as well as the corresponding plots, were computed using R software and the ade4 and made4 packages furnished by Bioconductor.[11]

[11] http://www.bioconductor.org

The Mann-Whitney test was used to select genes differentially expressed in normal mucosa and adenomas; Benjamini-Hochberg multiple testing correction was applied with a false discovery rate of 0.01. The genes in this set that were differentially expressed with fold differences of ≥2.0 were then analyzed with ErmineJ software (48) to identify any biological processes from the Gene Ontology database (49) that were overrepresented.

Pearson correlation was used to identify correlation between *KIAA1199* expression and the expression of other genes in the entire set of tissue samples. Fisher's exact test was used to identify possible overrepresentation of known Wnt targets among genes whose expression was closely correlated with that of *KIAA1199* (correlation values ≥0.8).

Reverse transcription-PCR and Northern blotting were done as previously described (46, 50) to verify the expression level of *KIAA1199* in tissue samples and in LS174T colon cancer cells in which inducible inhibition of the Wnt pathway had been achieved with previously described methods (14-16).

In situ *Hybridization*

Digoxigenin-labeled *KIAA1199* antisense riboprobes were synthesized from a PCR product amplified from human colon cDNA with *KIAA1199*-specific primers (sense: 5′-cacatcgggg-gaggagataga-3′; antisense, containing a T7 RNA polymerase-binding site: 5′-taatacgactcactatagggttccagacttgaca-3′). This product was transcribed *in vitro* using the DIG RNA labeling kit and T7 RNA polymerase (Roche Diagnostics). *In situ* hybridizations were done on paraffin-embedded sections of human colon fixed with 4% buffered formalin as described elsewhere (51).

Immunohistochemistry

Our *in silico* analysis of KIAA1199 (see Supplementary Data) indicated that residues 202 to 217 (IHSDRFDTYRSKKESE) form a loop between a conserved β-strand and the following helix of the NH_2-terminal GG domain. This charged, surface-exposed peptide was used to raise a rabbit polyclonal antibody, which was purified by affinity chromatography on Thiopropyl Sepharose 6B (Amersham) derivatized with the antigenic peptide. A 1:1,000 dilution of this antibody was used, as previously described (45), to evaluate KIAA1199 expression in formalin-fixed, paraffin-embedded sections of adenoma and normal mucosal tissues.

Acknowledgments

We thank the patients who participated in this study; R. Haider, E. Pani, T. Lehmann, A. Patrignani, and U. Wagner for technical assistance; A. Mueller, E. Veljkovic, and F. Bannwart for critical reading of the manuscript; and M. Kent for editorial assistance.

References

1. Winawer SJ, Zauber AG, Fletcher RH, et al. Guidelines for colonoscopy surveillance after polypectomy: a consensus update by the US Multi-Society Task Force on Colorectal Cancer and the American Cancer Society. Gastroenterology 2006;130:1872–85.

2. Stryker SJ, Wolff BG, Culp CE, Libbe SD, Ilstrup DM, MacCarty RL. Natural history of untreated colonic polyps. Gastroenterology 1987;93:1009–13.

3. Pinto D, Clevers H. Wnt, stem cells and cancer in the intestine. Biol Cell 2005; 97:185–96.

4. Korinek V, Barker N, Morin PJ, et al. Constitutive transcriptional activation by a β-catenin-Tcf complex in APC−/− colon carcinoma. Science 1997;275: 1784–7.

5. Morin PJ, Sparks AB, Korinek V, et al. Activation of β-catenin-Tcf signaling in colon cancer by mutations in β-catenin or APC. Science 1997;275:1787–90.

6. Update on the Paris classification of superficial neoplastic lesions in the digestive tract. Endoscopy 2005;37:570–8.

7. Jass JR. Classification of colorectal cancer based on correlation of clinical, morphological and molecular features. Histopathology 2007;50:113–30.

8. di Pietro M, Sabates Bellver J, Menigatti M, et al. Defective DNA mismatch repair determines a characteristic transcriptional profile in proximal colon cancers. Gastroenterology 2005;129:1047–59.

9. Ter Braak C. Canonical correspondence analysis: a new eigenvector technique for multivariate direct gradient analysis. Ecology 1986;67:1167–79.

10. Miki R, Kadota K, Bono H, et al. Delineating developmental and metabolic pathways *in vivo* by expression profiling using the RIKEN set of 18,816 full-length enriched mouse cDNA arrays. Proc Natl Acad Sci U S A 2001;98:2199–204.

11. Wu LF, Hughes TR, Davierwala AP, Robinson MD, Stoughton R, Altschuler SJ. Large-scale prediction of *Saccharomyces cerevisiae* gene function using overlapping transcriptional clusters. Nat Genet 2002;31:255–65.

12. Zhang W, Morris QD, Chang R, et al. The functional landscape of mouse gene expression. J Biol 2004;3:21.

13. Van der Flier LG, Sabates-Bellver J, Oving I, et al. The intestinal Wnt/TCF signature. Gastroenterology 2007;132:628–32.

14. van de Wetering M, Barker N, Harkes IC, et al. Mutant E-cadherin breast cancer cells do not display constitutive Wnt signaling. Cancer Res 2001;61: 278–84.

15. van de Wetering M, Sancho E, Verweij C, et al. The β-catenin/TCF-4 complex imposes a crypt progenitor phenotype on colorectal cancer cells. Cell 2002;111:241–50.

16. van de Wetering M, Oving I, Muncan V, et al. Specific inhibition of gene expression using a stably integrated, inducible small-interfering-RNA vector. EMBO Rep 2003;4:609–15.

17. Notterman DA, Alon U, Sierk AJ, Levine AJ. Transcriptional gene expression profiles of colorectal adenoma, adenocarcinoma, and normal tissue examined by oligonucleotide arrays. Cancer Res 2001;61:3124–30.

18. Lin YM, Furukawa Y, Tsunoda T, Yue CT, Yang KC, Nakamura Y. Molecular diagnosis of colorectal tumors by expression profiles of 50 genes expressed differentially in adenomas and carcinomas. Oncogene 2002;21: 4120–8.

19. Nosho K, Yamamoto H, Adachi Y, Endo T, Hinoda Y, Imai K. Gene expression profiling of colorectal adenomas and early invasive carcinomas by cDNA array analysis. Br J Cancer 2005;92:1193–200.

20. Lechner S, Muller-Ladner U, Renke B, Scholmerich J, Ruschoff J, Kullmann F. Gene expression pattern of laser microdissected colonic crypts of adenomas with low grade dysplasia. Gut 2003;52:1148–53.

21. Nata K, Liu Y, Xu L, et al. Molecular cloning, expression and chromosomal localization of a novel human REG family gene, REG III. Gene 2004;340:161–70.

22. Bishnupuri KS, Luo Q, Murmu N, Houchen CW, Anant S, Dieckgraefe BK. Reg IV activates the epidermal growth factor receptor/Akt/AP-1 signaling pathway in colon adenocarcinomas. Gastroenterology 2006;130:137–49.

23. Hanai J, Mammoto T, Seth P, et al. Lipocalin 2 diminishes invasiveness and metastasis of Ras-transformed cells. J Biol Chem 2005;280:13641–7.

24. Comijn J, Berx G, Vermassen P, et al. The two-handed E box binding zinc finger protein SIP1 downregulates E-cadherin and induces invasion. Mol Cell 2001;7:1267–78.

25. Jankowski JA, Bedford FK, Boulton RA, et al. Alterations in classical cadherins associated with progression in ulcerative and Crohn's colitis. Lab Invest 1998;78:1155–67.

26. Hardy RG, Tselepis C, Hoyland J, et al. Aberrant P-cadherin expression is an early event in hyperplastic and dysplastic transformation in the colon. Gut 2002; 50:513–9.

27. Lin SY, Elledge SJ. Multiple tumor suppressor pathways negatively regulate telomerase. Cell 2003;113:881–9.

28. Mariadason JM, Nicholas C, L'Italien KE, et al. Gene expression profiling of intestinal epithelial cell maturation along the crypt-villus axis. Gastroenterology 2005;128:1081–8.

29. Ding H, Schertzer M, Wu X, et al. Regulation of murine telomere length by Rtel: an essential gene encoding a helicase-like protein. Cell 2004;117:873–86.

30. Pitti RM, Marsters SA, Lawrence DA, et al. Genomic amplification of a

decoy receptor for Fas ligand in lung and colon cancer. Nature 1998;396:699–703.

31. Bai C, Connolly B, Metzker ML, et al. Overexpression of M68/DcR3 in human gastrointestinal tract tumors independent of gene amplification and its location in a four-gene cluster. Proc Natl Acad Sci U S A 2000;97:1230–5.

32. Postma C, Hermsen MA, Coffa J, et al. Chromosomal instability in flat adenomas and carcinomas of the colon. J Pathol 2005;205:514–21.

33. Thiebault K, Mazelin L, Pays L, et al. The netrin-1 receptors UNC5H are putative tumor suppressors controlling cell death commitment. Proc Natl Acad Sci U S A 2003;100:4173–8.

34. Dhanabal M, Jeffers M, LaRochelle WJ, Lichenstein HS. Angioarrestin: a unique angiopoietin-related protein with anti-angiogenic properties. Biochem Biophys Res Commun 2005;333:308–15.

35. Backlund MG, Mann JR, Holla VR, et al. 15-Hydroxyprostaglandin dehydrogenase is down-regulated in colorectal cancer. J Biol Chem 2005;280:3217–23.

36. Hogan MC, Griffin MD, Rossetti S, Torres VE, Ward CJ, Harris PC. PKHDL1, a homolog of the autosomal recessive polycystic kidney disease gene, encodes a receptor with inducible T lymphocyte expression. Hum Mol Genet 2003;12:685–98.

37. Nakayama M, Kikuno R, Ohara O. Protein-protein interactions between large proteins: two-hybrid screening using a functionally classified library composed of long cDNAs. Genome Res 2002;12:1773–84.

38. Tamagnone L, Artigiani S, Chen H, et al. Plexins are a large family of receptors for transmembrane, secreted, and GPI-anchored semaphorins in vertebrates. Cell 1999;99:71–80.

39. Comoglio PM, Tamagnone L, Giordano S. Invasive growth: a two-way street for semaphorin signalling. Nat Cell Biol 2004;6:1155–7.

40. Michishita E, Garces G, Barrett JC, Horikawa I. Upregulation of the KIAA1199 gene is associated with cellular mortality. Cancer Lett 2006;239:71–7.

41. Horikawa I, Parker ES, Solomon GG, Barrett JC. Upregulation of the gene encoding a cytoplasmic dynein intermediate chain in senescent human cells. J Cell Biochem 2001;82:415–21.

42. Abe S, Katagiri T, Saito-Hisaminato A, et al. Identification of CRYM as a candidate responsible for nonsyndromic deafness, through cDNA microarray analysis of human cochlear and vestibular tissues. Am J Hum Genet 2003;72:73–82.

43. Abe S, Usami S, Nakamura Y. Mutations in the gene encoding KIAA1199 protein, an inner-ear protein expressed in Deiters' cells and the fibrocytes, as the cause of nonsyndromic hearing loss. J Hum Genet 2003;48:564–70.

44. Marra G, Jiricny J. Multiple colorectal adenomas—is their number up? N Engl J Med 2003;348:845–7.

45. Truninger K, Menigatti M, Luz J, et al. Immunohistochemical analysis reveals high frequency of PMS2 defects in colorectal cancer. Gastroenterology 2005;128:1160–71.

46. di Pietro M, Marra G, Cejka P, et al. Mismatch repair-dependent transcriptome changes in human cells treated with the methylating agent *N*-methyl-*N*′-nitro-*N*-nitrosoguanidine. Cancer Res 2003;63:8158–66.

47. Benzécri J-P. Correspondence analysis handbook. New York: Marcel Dekker, Inc.; 1992.

48. Lee HK, Braynen W, Keshav K, Pavlidis P. ErmineJ: tool for functional analysis of gene expression data sets. BMC Bioinformatics 2005;6:269.

49. Ashburner M, Ball CA, Blake JA, et al. Gene ontology: tool for the unification of biology. The Gene Ontology Consortium. Nat Genet 2000;25:25–9.

50. Barker N, Hurlstone A, Musisi H, Miles A, Bienz M, Clevers H. The chromatin remodelling factor Brg-1 interacts with β-catenin to promote target gene activation. EMBO J 2001;20:4935–43.

51. Maake C, Auf der Maur F, Jovanovic K, Reinecke M, Hauri D, John H. Occurrence and localization of uroguanylin in the aging human prostate. Histochem Cell Biol 2003;119:69–76.

52. Kumar S, Tamura K, Nei M. MEGA3: integrated software for molecular evolutionary genetics analysis and sequence alignment. Brief Bioinform 2004;5:150–63.

Molecular Cancer Research

Transcriptome Profile of Human Colorectal Adenomas

Jacob Sabates-Bellver, Laurens G. Van der Flier, Mariagrazia de Palo, et al.

Mol Cancer Res 2007;5:1263-1275.